

Microscopic fracture mechanisms observed on Cu–Sn frangible bullets under quasi-static and dynamic compression

S. W. Banovic · S. P. Mates

Received: 25 October 2007 / Accepted: 5 May 2008 / Published online: 3 June 2008
© Springer Science+Business Media, LLC 2008

Abstract The damage behavior of Cu–Sn frangible bullets was characterized in an effort to aid predictions of impact performance of these projectiles with soft body armor through finite element simulations. Fracture surfaces and failed cross sections were examined via light optical and scanning electron microscopy and related to the composite bullet microstructure. Two types of samples were analyzed: (1) those used in quasi-static and dynamic diametral compression testing to determine the effective properties of the composite material, and (2) bullets discharged into soft body armor. Two primary microscopic fracture mechanisms were cleavage and intergranular fracture of the Cu–Sn intermetallic compounds, $\epsilon(\text{Cu}_3\text{Sn})$ and $\eta(\text{Cu}_6\text{Sn}_5)$, which joined the un-bonded copper particles in the composite microstructure. Microvoid coalescence of copper metal was also observed, though infrequently, in places where the spacing between intermetallic phase clusters on a single copper particle was typically no greater than 30 μm . These modes of failure were similar between the samples used in the mechanical testing methods and the discharged bullets. From these results, it is reasonable to assume that the failure strength data measured via diametral compression testing can be used to predict the onset of bullet failure on impact during finite element simulations.

Introduction

Frangible bullets have been marketed as lead-free alternatives for use at shooting ranges, during law enforcement training drills, and in situations where stray bullets or pass-throughs can cause catastrophic damage or unintended fatalities (i.e., nuclear facilities, airplanes, close quarter fighting). The design of a frangible bullet is such that the projectile disintegrates upon impact with a hard surface. In doing so, the small fragments quickly lose their kinetic energy and pose minimal threat to secondary targets (no ricochet or over-penetration). One variety of bullet is fabricated using powder metallurgy techniques to produce metal–matrix composites from mixtures of copper and tin powders [1]. After compressing and a low-temperature heat treatment, the microstructure consists of minor phase clusters containing Cu–Sn intermetallic compounds (IMCs), unreacted Sn, and porosity heterogeneously distributed throughout a Cu matrix [2]. The IMCs act as the binder between the copper powders, as the individual copper particles are not metallurgically bonded to each other.

Unlike Pb-base projectiles that are ductile and distribute their impact load over a relatively large area, the interaction of the frangible bullet, and in particular, the smaller fractured pieces, with soft body armor has not been adequately characterized. To fill this need, the Office of Law Enforcement Standards (OLEES) at the National Institute of Standards and Technology (NIST), under direction from the Department of Justice's National Institute of Justice (NIJ), is evaluating the relationship and performance of frangible bullets against personal body armor. A portion of this work involves finite element simulations of frangible bullet impacts against soft body armor to help develop improved body armor standards for law enforcement safety. These simulations depend on accurate knowledge of the mechanical properties and

S. W. Banovic (✉) · S. P. Mates
Metallurgy Division, National Institute of Standards
and Technology, Technology Administration, US Department
of Commerce, Gaithersburg, MD 20899, USA
e-mail: sbanovic@nist.gov

fracture behavior of the bullet materials at high loading rates. Toward this end, diametral compression tests were performed over various loading rates to determine the tensile strength of the bullet material and its sensitivity to strain rate for use in the computer models [3]. To complement this work, fractography and examination of failed cross sections of these samples and those discharged into soft body armor was conducted to resolve the microscopic fracture mechanisms of the material under these different testing conditions. It is imperative that the damage modes of the test samples and those of the bullets discharged into soft body armor be compared to resolve whether the fracture mechanisms are similar. Otherwise, uncertainty may exist that the tensile strength data derived from the diametral compression test are appropriate for use in modeling bullet penetration into soft body armor. This article discusses these findings and compares the failure modes observed on the various samples.

Experimental procedure

This analysis used 9 mm, 7.12 g (110 grain), Cu–Sn frangible bullets purchased from a commercial supplier. While a detailed description of the bullet thermomechanical history and resulting microstructure is given by Banovic [2], it will be briefly reviewed here and in section “Bullet microstructure”. Copper and tin powders, with sizes of approximately 8% greater than 250 mesh, approximate 30% greater than 325 mesh, and the balance less than 325 mesh, were blended together in a 9:1 ratio, respectively, by weight percent. A small amount of zinc stearate lubricant was used to aid in compaction and ejection of the green compact. Bullet-shaped green bodies were produced using a standard straight-walled die situated in a mechanical press under approximately 20 tons of pressure. The green bodies were removed from the mold and given a low-temperature heat treatment of 260 °C for 30 min under a nitrogen atmosphere and allowed to cool to room temperature. The average diameter, length, and mass of the bullets were 9.02 mm, 16.90 mm, and 7.09 g, respectively. Bullets were chosen at random for testing from multiple procurements.

Metallography

A high-speed saw with ceramic blade was used to section the bullets for metallographic examination. Portions of the bullets were mounted in cold setting epoxy and standard metallographic procedures were used to prepare the samples for evaluation. A solution of 3 g FeCl₃, 50 mL of water, 25 mL of HCl, and 100 mL of ethanol was used to reveal the structure.

Mechanical methods

Two techniques generated mechanical fracture in the samples. The first was the diametral compression test [4]; also known as the Brazilian disk test, a disk-shaped sample is loaded in compression at two opposite points. The loading produces a region of nearly uniform tensile stress perpendicular to the load axis that is sufficient to fracture the specimen. Individual disks were cut from the bullets using a wire electrical discharge machining process, one disk per bullet, with a thickness of 4.5 mm. Quasi-static displacement rate tests were conducted on a servohydraulic loading machine with a constant ram velocity of 0.001 mm/s. For the majority of tests, the actuator was immediately retracted upon primary specimen failure. A few tests were allowed to continue past failure until the specimen fractured in to two for observation of the fracture surface. Dynamic tests were conducted using a Kolsky bar technique [5] with a displacement rate of approximately 12.5 m/s. Finite element simulations were performed to aid specimen design and to analyze the stress in the specimen at failure to obtain the most accurate possible failure strength measurement [3].

Secondly, as-received bullets were discharged from a bench-mounted gun platform located on the NIST campus in Gaithersburg, MD. For these tests, a 10-in. long barrel that meets the American National Standards Institute (ANSI)/Small Arms and Ammunition Manufactures Institute (SAAMI) specifications for a 9-mm Luger velocity test barrel was employed. The muzzle velocity of the bullets ranged from 367 to 390 m/s (1204–1281 ft/s) with an average of 375 m/s. The target was a field-returned, soft body armor vest, a model that was certified to NIJ Standard-0101.03 [6], with a clay backing.

Fractography

Fractography was conducted using a scanning electron microscope (SEM) with a LaB₆ filament. The accelerating voltage was 20 kV with working distances ranging from 15 to 25 mm.

Results

Bullet microstructure

Description and development of the bullet microstructure was previously discussed by Banovic [2] with a brief narrative given here. Figure 1a shows heterogeneous distribution of the minor phase clusters and porosity in the copper matrix; these clusters consist of ϵ (Cu₃Sn), η (Cu₆Sn₅), and un-reacted Sn, Fig. 1b. Approximately 5%

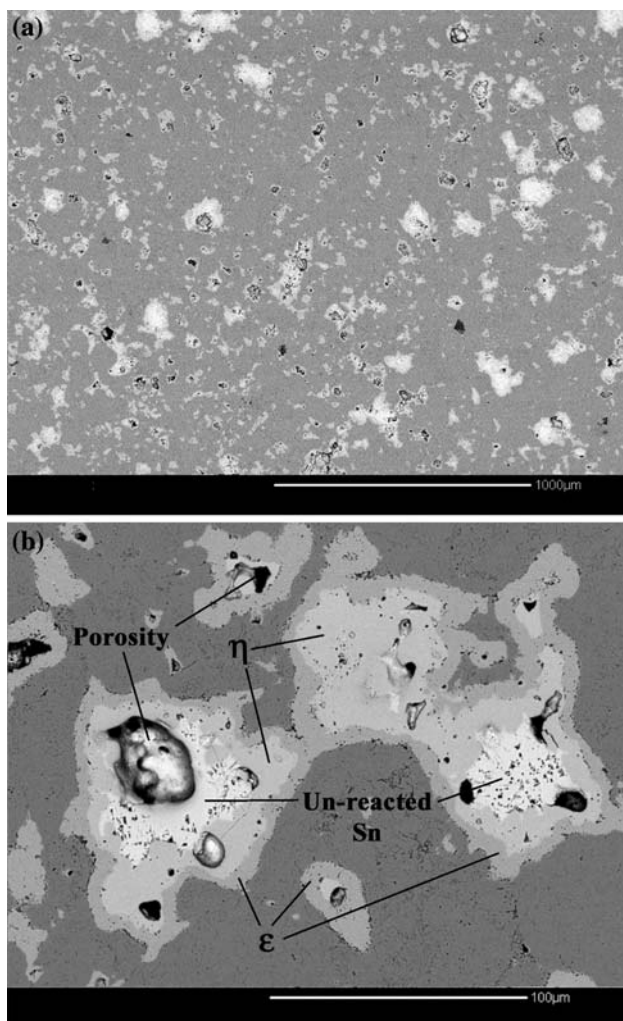


Fig. 1 Back-scattered electron images of the microstructure from a polished Cu–Sn frangible bullet. **(a)** Heterogeneous distribution of minor phase cluster (light gray/white) and porosity (black) and **(b)** individual phases in the copper matrix

porosity is encased within these clusters. Neither the porosity nor the intermetallic compounds (IMCs) were interconnected.

Individual copper particles of the Cu matrix are clearly seen in the etched microstructure, Fig. 2. While not quantitatively evaluated, a wide range of particle sizes appear to have been used. Of note is that the individual copper particles are not metallurgically bonded to each other, but rather, are held together by the Cu–Sn IMC phases that form a brittle network between the copper powders. No intact tin particles were observed, as they were transformed into a transient liquid that wetted the copper particle boundaries during the low-temperature heat treatment to form the IMCs. Etching of the IMC phases showed that ϵ (Cu₃Sn) consisted of fine-grained platelets and η (Cu₆Sn₅) was composed of large nodular grains, Fig. 3.

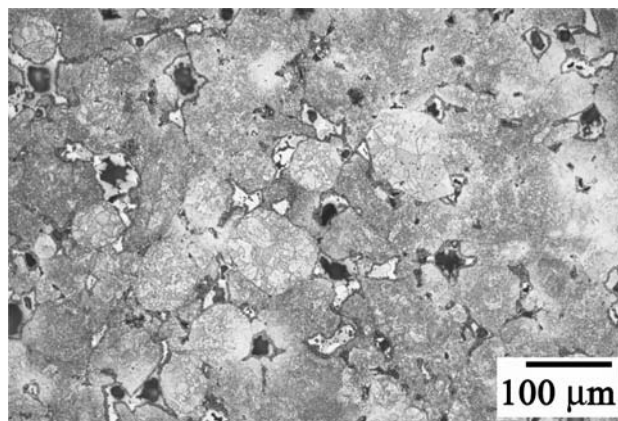


Fig. 2 Optical micrograph showing the individual copper particles of the Cu matrix and the minor phase clusters (light gray with dark gray border). Sample was etched

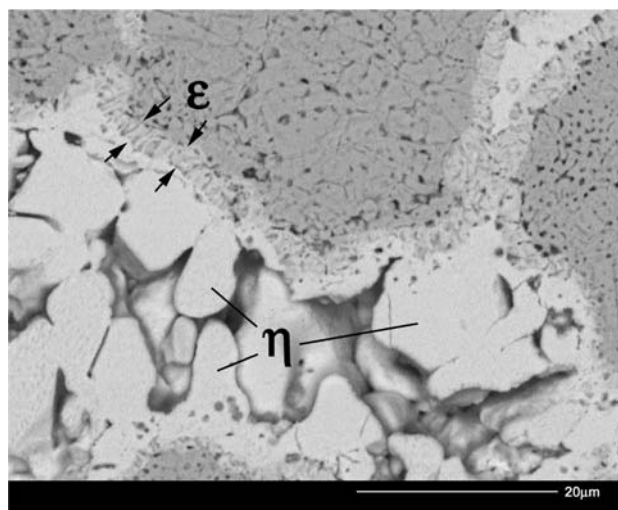


Fig. 3 Back-scattered electron image showing the microstructures of the IMCs. Sample was etched

Mechanical properties

The tensile fracture stress of the material, as obtained from the diametral compression tests, is 104 ± 14 MPa. The fracture stress is deduced by computing the tensile stresses produced by the diametral load at failure, as indicated in Fig. 4. The compressive yield strength of this material is 2.5 times higher, indicating the brittle nature of the material. Neither the compressive or tensile strength of the material was very sensitive to strain rate. Further details on the mechanical behavior of the material, including the stress analysis used to determine tensile strength from the diametral test data, can be found in Mates et al. [3].

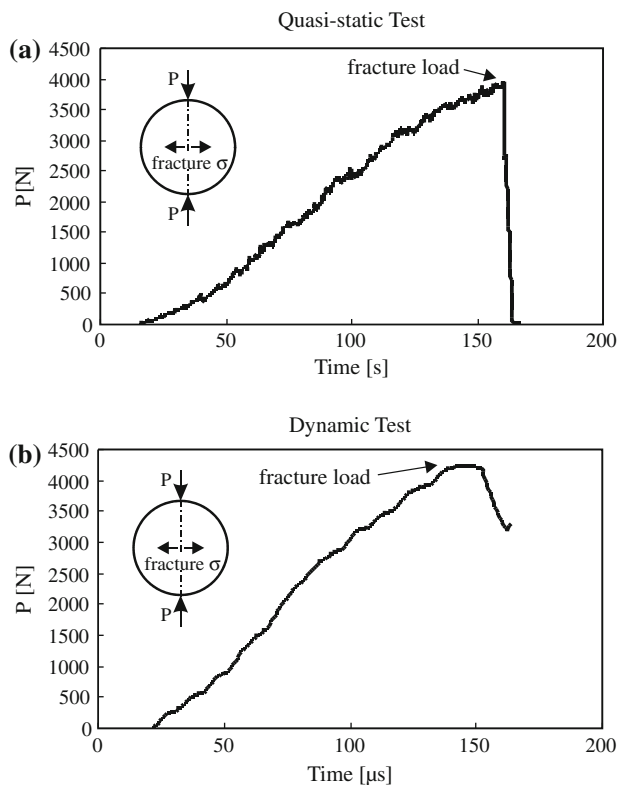


Fig. 4 Load vs. time data obtained from (a) quasi-static and (b) dynamic diametral compression tests

Macroscopic description of failure

The samples had different macroscopic responses to the mechanical testing methods. Table 1 is provided to summarize both macroscopic and microscopic damage observations. For the diametral compression samples, fracture occurred on a well-defined plane parallel to the loading

direction. Quasi-static samples developed a single crack that did not propagate across the entire sample, unless the test was intentionally continued past primary specimen failure to produce an observable fracture surface. Similarly, dynamic samples developed a primary fracture plane parallel to the loaded diameter that resulted in two large portions with numerous small bits and some powder scattered around the sample, Fig. 5a.

For the bullets discharged into the soft body armor, fracture occurred on multiple planes throughout the sample. Pieces returned for analysis were typically from one quarter to one third of the original bullet, Fig. 5b. These portions did not penetrate the vest. The remaining pieces of the bullets were either embedded in the vest or in the clay backing and were considered irretrievable.

Fractography

The most common characteristic observed on all fracture surfaces was separation at the copper particle interfaces, whether in the form of partial separation between two particles, Fig. 6a, or complete pull-out of the powder, Fig. 6b. Another form of copper matrix failure was microvoid coalescence (MVC), typically found when the copper matrix was closely bounded by IMC clusters, Fig. 7. On average, the intercluster distance of the IMCs was characteristically less than 30 μm. While some instances were observed on dynamic samples and discharged bullets, this feature was most often seen on fracture surfaces from the quasi-static samples.

Cleavage of the IMCs was also readily observed on all samples, Fig. 8a and b, with Fig. 8c showing intergranular fracture of the large η(Cu₆Sn₅) grains.

Porosity observed on the fracture surface had two different morphologies. The first, Fig. 9a, was similar in size

Table 1 Summarized description of damage characteristics for each test

Damage description	Quasi-static testing	Dynamic testing	Bullet testing
Macroscopic fracture	– single fracture – well-defined plane – plane parallel to loaded diameter – did not propagate across entire sample	– single fracture – well-defined plane – plane parallel to loaded diameter – fractured sample in to two	– multiple fractures – multiple planes – planes have no specific orientation – sample in multiple pieces of various size
Copper particle separation	Common	Common	Common
Microvoid coalescence of copper	Common	Rare	Rare
Cleavage of Cu–Sn IMCs	Common	Common	Common
Intergranular fracture of Cu–Sn IMCs	Common	Common	Common
Porosity	Typically unaffected	Unaffected and compressed	Typically compressed
Sliding scars	Absent	Near end caps	Common
Subsurface deformation	Absent	Up to 500 μm below fracture surface	Widespread

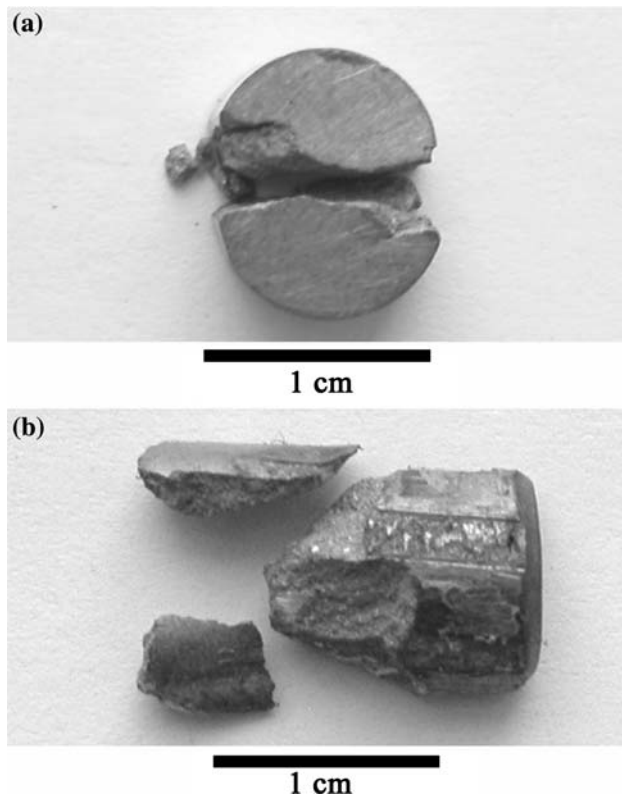


Fig. 5 Characteristic macroscopic failures of tested samples: (a) dynamic samples and (b) recovered pieces from discharged bullet

and shape to that in the polished cross section of untested material with the second being compressed, Fig. 9b. The latter was most prevalent in the discharged bullets.

Sliding scars were also observed on the samples tested at higher loading rates, Fig. 10. The discharged bullets had the highest occurrence of this feature with over half of the fracture surface experiencing this attribute. Scars observed on the dynamic samples were concentrated solely near the ends of the sample in contact with the test mandrels, whereas the central portion of the specimen was unaffected.

Metallography of failed samples

Metallographically polished samples of the failed materials were also examined. Figure 11 shows a cross section of a fracture in a quasi-static sample. The crack primarily followed particle–particle boundaries and through fractured IMC phases, Fig. 11b. Below the fracture surface, little if any damage was observed in the copper matrix or the IMCs. Similar results were observed for the dynamic samples; however, damage of the material (copper particle boundary separation, fracture of the IMC) was noted up to 500 μm beneath the fracture surfaces, Fig. 12. Metallographic examination of the bullet fired into the body armor

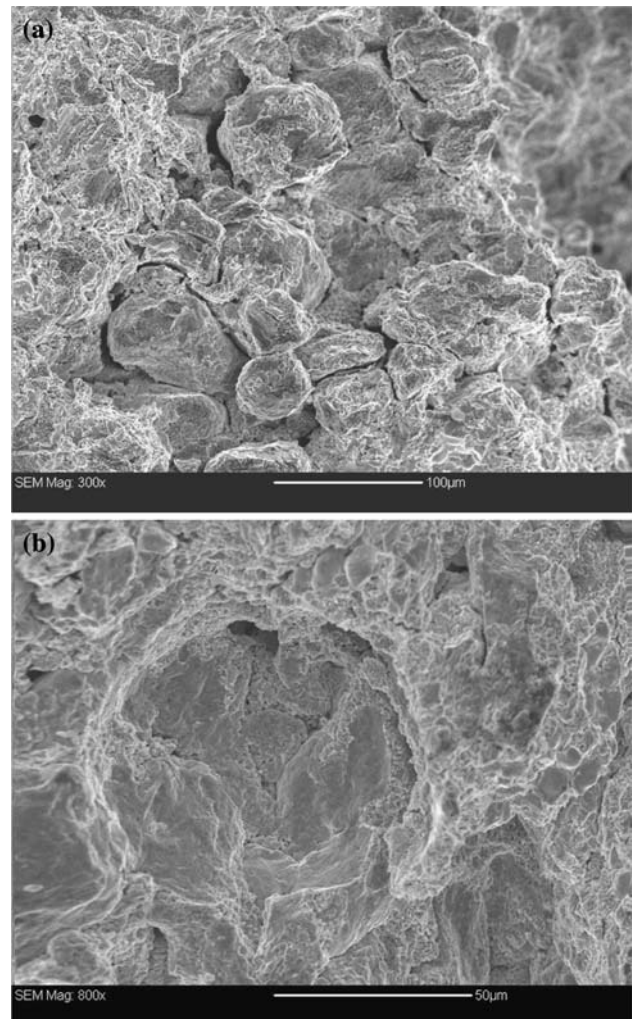


Fig. 6 Secondary electron micrographs showing separation of unbonded copper particles. (a) Partial separation of copper particles (from dynamic sample) and (b) complete particle removal of particle from the matrix (from discharged bullet)

revealed that particle boundary separation and IMC fracture occurred extensively throughout the entire sample, Fig. 13.

Discussion

To accurately predict the fracture behavior of Cu–Sn frangible bullets when striking soft body armor through finite element simulations, the mechanical properties, failure strength, and fracture mechanisms must be evaluated under test conditions similar to those experienced by the impacting bullet. Toward this end, diametral compression testing, under quasi-static and high loading rates, was conducted to determine the tensile properties of the composite material. This work was reported by Mates et al. [3]. However, it is imperative that the damage modes of the

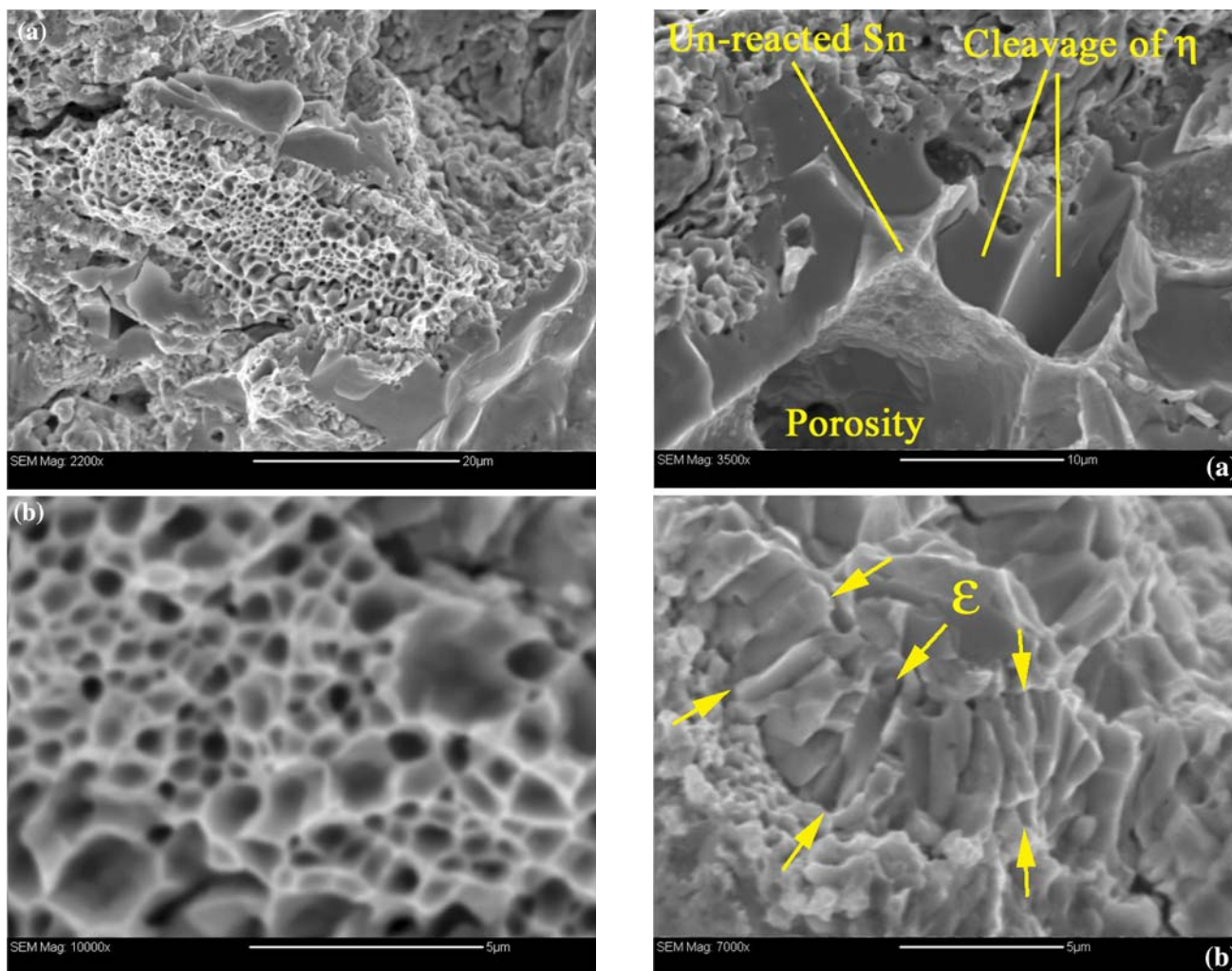


Fig. 7 Secondary electron micrograph showing microvoid coalescence of the copper metal (from quasi-static sample)

test samples and those of the bullets discharged into soft body armor be compared to resolve whether the fracture mechanisms are similar. Otherwise, uncertainty may exist that the tensile strength data derived from the diametral compression test are appropriate for use in modeling bullet penetration into soft body armor.

Failure of the diametral compression samples occurred via cleavage and intergranular fracture of the IMCs, Fig. 8, in conjunction with copper particle–particle boundary separation, Fig. 6. The former is a low-energy failure mode that results in the frangible nature of the bullet upon impact with a hard target. The IMC phases are formed to act as a brittle binder between the un-bonded copper particles. These phases develop during a low-temperature heat treatment in which a transient liquid Sn film wets the copper powder interfaces, allowing for Cu diffusion into the liquid, and subsequent growth of the ϵ (Cu₃Sn) and η (Cu₆Sn₅) phases [2]. The development of these IMCs

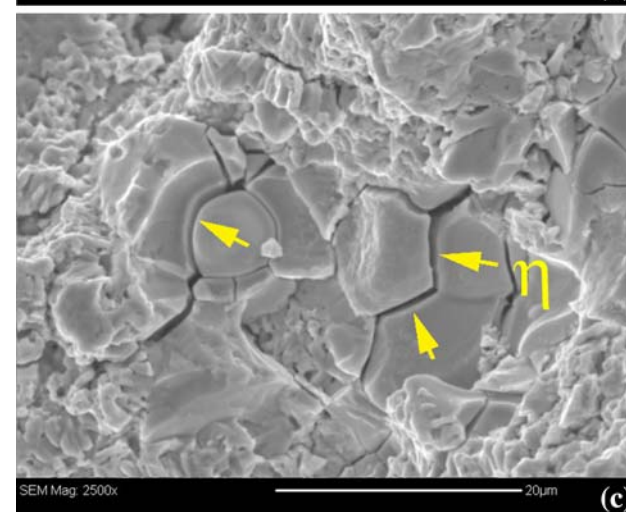


Fig. 8 Secondary electron micrographs showing (a) cleavage of η (from dynamic sample), (b) cleavage of ϵ (from discharged bullet); (c) intergranular fracture of η (from discharged bullet)

permits the bullet to have sufficient strength during firing of the ammunition (particle adherence as a result of the intermetallic binder), but disintegrate upon impact with a

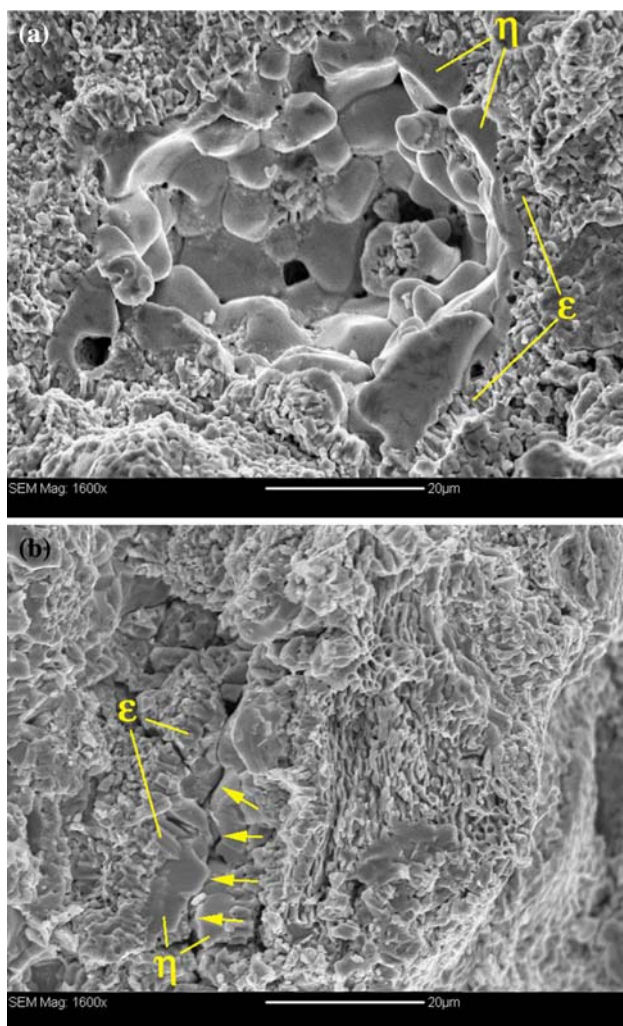


Fig. 9 Secondary electron micrographs of porosity surrounded by fractured IMCs. (a) Porosity similar to the as-received state (from dynamic sample) and (b) collapsed porosity (from discharged bullet)

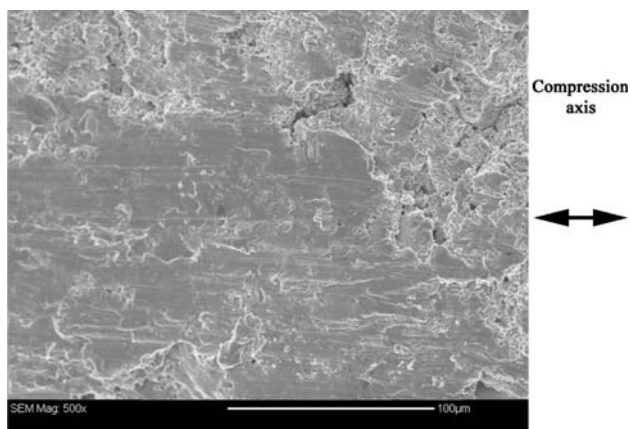


Fig. 10 Secondary electron micrograph of a sliding scar (from discharged bullet)

rigid surface (due to the low fracture toughness of the intermetallic).

However, it is essential that metallurgical bonding of the copper particles does not occur during the low-temperature heat treatment. If the copper powders sinter, the material will behave as a ductile mass and the frangibility of the bullet will be lost. With un-bonded interparticle boundaries, cracks that form in the brittle IMCs can easily extend along these predisposed imperfections in the structure. Further, there does not appear to be any interlocking of the copper particles that would represent a mechanical bond between particles, Fig. 2. Thus, once the IMC bonding is severed along a plane, the structure disintegrates.

Although infrequent, microvoid coalescence (MVC) of the copper metal was a third failure mechanism. This higher energy mode was observed only when the inter-cluster distance of the IMCs was short, typically less than 30 μm . From all appearances, this mechanism occurred only in single copper particle when IMCs formed on opposite sides of a particle. Deforming material with the closely spaced IMC phases resulted in the development of high local plastic strains in the copper metal which lead to the evolution of ductile regions with fine, near-featureless, near-equiaxed dimples closely bounded by the fractured IMC. The shape of the dimples suggests that the material failed under simple uniaxial loading conditions, as they appear to grow out of the plane normal to the stress axis. As MVC was rare, its contribution to failure was insignificant.

Comparison of the mechanically tested samples with those of the discharged bullets showed similar damage features. Cleavage and intergranular fracture of the intermetallic phases were readily observed on all samples, as were copper particle boundary separation and pull out of individual powders. Unfortunately, a fair amount of secondary damage (scars/abrasions) occurred on the fracture surface of the discharged bullets that obliterated the primary damage related to failure. This was most likely a result of sliding contact between individual portions of the fractured material. Therefore, quantitative analysis of the fracture mechanisms was not conducted as large, undamaged regions were unavailable to be used as representative areas of interest on the bullet samples. Regardless, enough unscarred fracture surface existed to allow the qualitative assessment that the primary fracture modes observed in the discharged bullets were similar to those observed in the mechanically tested samples.

Cross sections of failure surfaces revealed that subsurface damage differed between the compression tests and the test-fired samples; there was also a slight difference noted between the quasi-static and dynamic samples. For the discharged bullets, interparticle separation and fracture of the IMCs was extensively observed throughout the

Fig. 11 Light optical micrograph of the fracture from a quasi-static sample. Crack primarily follows along particle–particle boundaries or through fracture of the IMC as seen in (b). Direction of loading is parallel to the crack

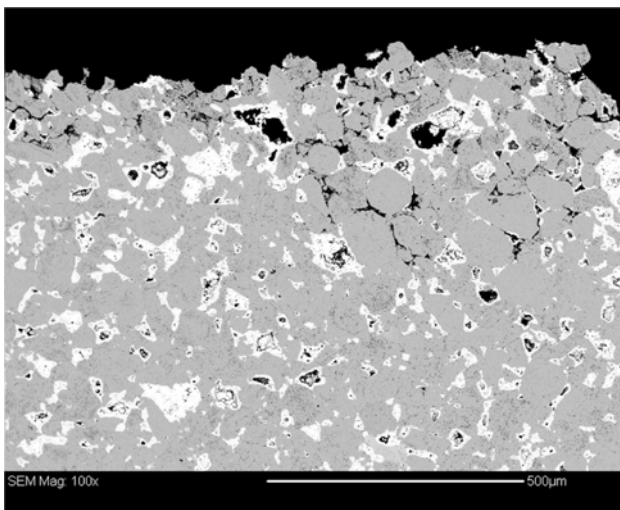
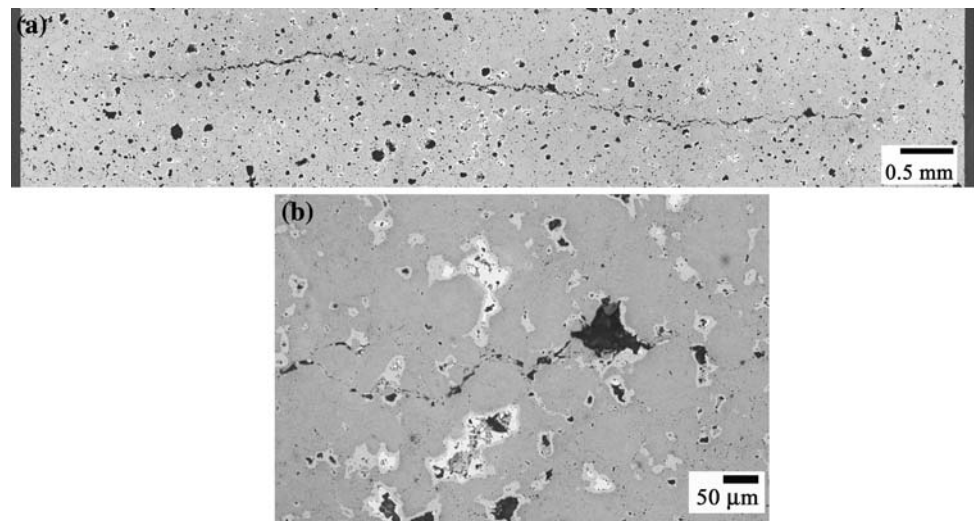


Fig. 12 Scanning electron micrograph of the fracture from a dynamic sample. Cracking also follows along particle–particle boundaries or through fracture of the IMC. Deformation of the material was found as much as 500 μm from the fracture surface. Direction of loading is parallel to the fracture surface

sample, Fig. 13. For the diametral compression samples, failure of the quasi-static samples was associated solely with the fracture surface, Fig. 11, whereas the dynamic test resulted in more widespread damage beneath the fracture surface, Fig. 12. The difference in damage to the structure may be related to (1) the amount of energy introduced to the bullet, (2) the stress state experienced by the different sample geometries (discussion of this factor is outside the scope of this paper and will be covered in a subsequent work), (3) stress wave effects in discharged bullets, and (4) the number of “loadings” experienced by the sample.

During mechanical testing of the bullet material or when the bullet strikes a solid target, energy is introduced into the material. The amount of energy imparted to the samples during diametral compression testing was computed by

integrating load–displacement data obtained from the tests. Calculated energies were similar between the quasi-static and dynamic tests, approximately 0.3 J. The amount of energy introduced to the discharged bullet was calculated from the kinetic energy E of the system:

$$E = \frac{1}{2}mv^2 \quad (1)$$

where m is the mass of the bullet and v is muzzle velocity. Using the average values stated in section “Experimental procedure”, approximately 500 J was imparted to the bullet upon impact with the soft body armor. Taking into consideration the volume of the samples, there was approximately two orders of magnitude difference in *energy per unit volume* between diametral compression samples and the discharged bullets. It is the dissipation of this extra energy, in combination with the stress state imposed upon the sample, that is partially responsible for the widespread failure of the brittle IMCs observed in the bullet samples. Further, stress wave effects in the test-fired bullet will have a significant influence on the damage sustained by the material on impact. In the quasi-static case, stresses are in equilibrium up until failure, after which the stress rapidly relaxes, preventing further material damage throughout the rest of the sample. In a bullet-impact event, stress waves travel so quickly that stress relaxation remains localized, resulting in multiple failure sites and fragmentation of the material [7]. Thus a greater degree of particle separation occurs in the test-fired bullet.

The minor difference between the diametral compression test samples (width of damage zone) can be explained by the number of “loadings” that the samples experienced. During the quasi-static testing, the actuator provided a single, continuous loading which was immediately removed upon primary specimen failure. In the dynamic tests, the sample was subjected to multiple loadings beyond the initial fracture due to residual elastic energy trapped in

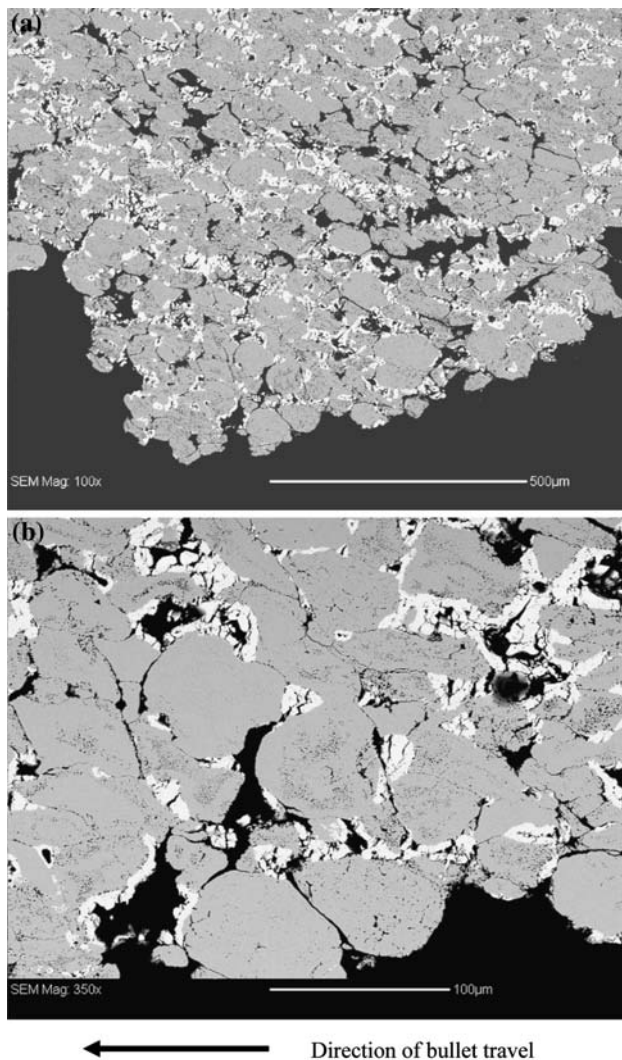


Fig. 13 Scanning electron micrographs of fracture in a discharged bullet sample taken from failure along the side of the bullet near the front end. Extensive particle separation and IMC fracture was observed throughout the sample

the bars. It is possible that the large damage zones observed in the dynamically tested samples are the result of these multiple impacts.

Despite the observed difference in width of the damage zone between the quasi-static and dynamic samples, however, the load at failure and the associated stress conditions were approximately equal in the two cases [3]. The stress conditions and loading rates experienced by the discharged bullets differ significantly from the diametral compression

test apparatus, leading to the more complicated fracture/damage characteristics observed here. Regardless of these differences, the similarities in fracture mechanisms observed suggest that the failure strength data determined by the diametral compression test are valid for modeling purposes to predict the onset of bullet failure on impact.

Conclusion

The mechanical failure and damage response of Cu–Sn frangible bullets were evaluated from, and compared between, different mechanical testing methods and discharged bullets. The main fracture mechanism was cleavage and intergranular fracture of the two Cu–Sn intermetallic compound phases that provided the brittle connective network between the un-bonded copper particles. Fracture modes between all samples were similar, though the microstructure experienced significantly more damage in samples tested at higher loading rates (dynamic testing and bullet impacts). From these results, it is reasonable to assume that the failure strength data determined by the diametral compression test can be used to predict the onset of bullet failure on impact during finite element simulations.

Acknowledgements This work was supported by the Office of Law Enforcement Standards at NIST and the National Institute of Justice at the Department of Justice. The discharged bullets were tested and obtained with the help of M. Riley and N. Waters. *Disclaimer:* Identification of any product in this manuscript does not imply recommendation or endorsement by NIST, the Department of Commerce, or the U.S. Government, nor does it imply that the identified product is the best available.

References

1. United States Patent 6,090,178. July 18, 2000. Frangible metal bullets, ammunition, and method of making such articles (Inventory is Joseph C. Benini)
2. Banovic SW (2007) Mater Sci Eng A 460–461:428. doi:[10.1016/j.msea.2007.01.113](https://doi.org/10.1016/j.msea.2007.01.113)
3. Mates SP, Rhorer R, Banovic S, Whitenton E, Fields RJ (2008) Int J Impact Eng 35(6):511. doi:[10.1016/j.ijimpeng.2007.04.005](https://doi.org/10.1016/j.ijimpeng.2007.04.005)
4. Rudnick A, Hunter AR, Holden FC (1963) Mater Res Stand 3:283
5. Gray GT III (1990) ASM handbook, vol 8. The American Society for Metals, Materials Park, OH, pp 462–476
6. National Institute of Justice (1987) Ballistic resistance of police body armor. NIJ Standard-0101.03
7. Meyers MA (1994) Dynamic behavior of materials. John Wiley & Sons, New York